Development 135, 1781-1790 (2008) doi:10.1242/dev.013847

MALS-3 regulates polarity and early neurogenesis in the developing cerebral cortex

Karpagam Srinivasan[1], Jason Roosa[1], Olav Olsen[2], Soung-Hun Lee[1], David S. Bredt[3] and Susan K. McConnell[1,*]

Apicobasal polarity plays an important role in regulating asymmetric cell divisions by neural progenitor cells (NPCs) in invertebrates, but the role of polarity in mammalian NPCs is poorly understood. Here, we characterize the function of the PDZ domain protein MALS-3 in the developing cerebral cortex. We find that MALS-3 is localized to the apical domain of NPCs. Mice lacking all three MALS genes fail to localize the polarity proteins PATJ and PALS1 apically in NPCs, whereas the formation and maintenance of adherens junctions appears normal. In the absence of MALS proteins, early NPCs progressed more slowly through the cell cycle, and their daughter cells were more likely to exit the cell cycle and differentiate into neurons. Interestingly, these effects were transient; NPCs recovered normal cell cycle properties during late neurogenesis. Experiments in which MALS-3 was targeted to the entire membrane resulted in a breakdown of apicobasal polarity, loss of adherens junctions, and a slowing of the cell cycle. Our results suggest that MALS-3 plays a role in maintaining apicobasal polarity and is required for normal neurogenesis in the developing cortex.

KEY WORDS: MALS, LIN7, Apicobasal polarity, Neurogenesis, Proliferation

INTRODUCTION

Neural progenitor cells (NPCs) in the cortical ventricular zone (VZ) are inherently polarized, with distinct cellular structures (cilia, centrosomes and adherens junctions) and molecular factors (Numb) localized apically (Aaku-Saraste et al., 1996; Astrom and Webster, 1991; Chenn et al., 1998; Zhong et al., 1996). This intrinsic polarity is exploited when NPCs undergo asymmetric mitotic divisions to produce apical and basal daughters with different cell fates (Chenn and McConnell, 1995; Chenn et al., 1998; Gotz and Huttner, 2005; Huttner and Kosodo, 2005). Imaging studies reveal that the apical cell surface is distributed unequally during asymmetric division of NPCs, suggesting that apically localized molecules might play a crucial role in determining the fates and mitotic behaviors of newly generated daughter cells (Huttner and Kosodo, 2005; Kosodo et al., 2004).

The fate of daughter cells that retain apical components remains controversial. Some studies suggest that these cells continue to proliferate and remain as NPCs (Miyata et al., 2001), whereas other studies suggest that they differentiate into neurons (Huttner and Kosodo, 2005; Kosodo et al., 2004; Wodarz and Huttner, 2003). Despite this disagreement, it is clear that only one daughter of an asymmetric division inherits apical components, and that this daughter has a fate distinct from that of the other (Miyata et al., 2001; Noctor et al., 2001). These observations suggest that determinants at the apical membrane [such as PAR6 (PARD6A – Mouse Genome Informatics) and PAR3 (PARD3 – Mouse Genome Informatics)] or associated with adherens junctions might influence the fates of daughter cells (Cappello et al., 2006; Imai et al., 2006).

Numerous proteins, including Numb, PAR3, CDC42, prominin 1 (CD133), ASPM and afadin (MLLT4 – Mouse Genome Informatics), are localized apically in NPCs (Gotz and Huttner, 2005), and many of these play crucial roles in corticogenesis by regulating apicobasal polarity (Fish et al., 2006; Junghans et al., 2005; Petersen et al., 2002). For example, conditional disruption of *CDC42* causes a loss of apical markers and adherens junctions in NPCs, which become mislocalized to the basal VZ and show altered fates and mitotic behavior (Cappello et al., 2006). The brains of transgenic mice that overexpress the junctional protein β-catenin are much larger than those of wild-type mice, because of an increase in the number of cycling progenitors (Chenn and Walsh, 2003), whereas loss of the basally localized protein LGL results in severe brain dysplasia and proliferation defects during corticogenesis (Klezovitch et al., 2004). These studies suggest that the establishment and maintenance of polarity in NPCs is crucial to normal corticogenesis.

Studies in MDCK cells have identified three complexes (CRB3/PALS1/PATJ, PAR3/PAR6/aPKC and MALS/PALS1) that are crucial for maintaining polarity (Margolis and Borg, 2005). MALS (also known as LIN-7 or Veli) is a PDZ domain-containing protein that specifies cell fates in *C. elegans* by controlling the basal localization of the EGF receptor LET-23 in vulval precursor cells (Kaech et al., 1998). LET-23 is mislocalized to the apical membrane in *lin-7* mutants, leading to a mis-specification of vulval cell fates (Kaech et al., 1998). In vertebrates, there are three MALS genes, *MALS-1*, *-2* and *-3*. Silencing *MALS-3* (*LIN7C* – Mouse Genome Informatics) in MDCK cells results in defective tight junctions and the loss of several MALS-3 binding partners, such as PALS1 (Margolis and Borg, 2005; Olsen et al., 2005a). PALS1 (MPP5 – Mouse Genome Informatics) forms a complex with CRB3 and PATJ (INADL – Mouse Genome Informatics), and can also interact with PAR6, thus linking the PAR6 signaling complex to other apically localized proteins such as CRB3 and MALS-3 (Roh et al., 2002). Together, these proteins are positioned apically to link transmembrane signaling proteins with cytoskeletal structures and/or cell nuclei (Roh and Margolis, 2003).

Despite progress in understanding the role of MALS proteins in MDCK cells in vitro, less is known about their roles in vivo. MALS-1 and MALS-2 are expressed at synapses (Misawa et al., 2001), but *MALS-1/MALS-2* double knockout mice upregulate *MALS-3* and show no obvious synaptic defects (Misawa et al., 2001). The analysis of mice lacking all three MALS genes revealed that MALS

[1]Department of Biological Sciences, Stanford University, Stanford, CA 94305, USA. [2]Department of Physiology, University of California, San Francisco, San Francisco, CA 94143, USA. [3]Lilly Research Laboratories, Indianapolis, IN 46285, USA.

*Author for correspondence (e-mail: suemcc@stanford.edu)

Accepted 13 March 2008

proteins play a crucial role in presynaptic vesicle recycling; the triple knockout (TKO) resulted in reduced synaptic transmission and neonatal lethality (Olsen et al., 2005a; Olsen et al., 2006). Here, we explore these proteins in NPCs and find that MALS-3 is localized to the apical surface of progenitors during neurogenesis, where it interacts primarily with PALS1 and CASK (LIN-2). Analyses of *MALS*^{TKO} embryos revealed that MALS-3 is required for the normal regulation of NPC proliferation and differentiation at the onset of neurogenesis, and for the continued apical localization of PATJ and PALS1 proteins.

MATERIALS AND METHODS

In situ hybridization and immunohistochemistry

In situ hybridization was performed as described previously (Chen et al., 2005). Polyclonal antibodies were generated by immunizing rabbits (BAbCo Laboratories, Berkeley, CA) with full-length MALS-3 or Mint protein in BL21 pLysS. MALS-3 antibodies were affinity-purified using MALS-3-GST fusion proteins coupled to Affi-Gel 10 beads (Bio-Rad Laboratories, CA). Immunohistochemistry (IHC) was performed as described previously (Cappello et al., 2006). Other antibodies used were as follows (dilutions used for IHC are given first, those for western blots (WB), second): MALS (LIN-7; Ben Margolis, University of Michigan, Ann Arbor, MI; 1:2000; 1:5000), PALS1 (Ben Margolis; 1:500; 1:2000), CRB3 (Ben Margolis; 1:500; 1:2000), ZO1 (Zymed, Invitrogen, Carlsbad, CA; 1:100; 1:500), ZO2 (Zymed; 1:100; 1:500), β-catenin (BD Transduction Laboratories, San Jose, CA; 1:200; 1:8000), DLG (BD Transduction Laboratories; 1:250; 1:500), α-catenin (BD Transduction Laboratories; 1:250; 1:250), pan-cadherin (SIGMA, St. Louis, MO; 1:250; 1:250), PATJ (Andre Le Bivic, Université de la Méditerranée, Marseille, France; 1:100; 1:500), CASK (Upstate Biochemicals, Waltham, MA; 2 μg/ml; 1 μg/ml), PAR6 (James Nelson, Stanford, CA; WB 1:50) TGN38 (ABCAM, Cambridge, MA; WB 1:500), Actin (Chemicon, Billerica, MA; WB 1:1000), α3-subunit of Na^+/K^+ ATPase (James Nelson; WB 1:500).

Cell fractionation and western analysis

Dorsal telencephalon was dissected from E14 rat embryos and homogenized in CSK homogenization buffer (50 mM NaCl, 150 mM sucrose, 10 mM Pipes, pH 6.8, 3 mM $MgCl_2$ with 1× Sigma protease inhibitor) by sonication on ice for 2 minutes, at 20% duty cycle, power setting 3. Cellular debris was removed by centrifugation at 1000× ***g*** for 10 minutes at 4°C.

High-speed centrifugation was used to pellet membranes and membrane-associated protein from the postnuclear supernatant (PNS), and to separate Triton X-100-soluble material from Triton X-100-insoluble material in the membrane pellet. Dorsal telencephalon from 10 E14 embryos was homogenized in 2 ml CSK or 2 ml CSK sans Mg^{+2} supplemented with EDTA. PNS (1 ml) was centrifuged at 100,000× ***g*** for 40 minutes to pellet membranes. The supernatant (S100) was removed and the pellet resuspended in an equal volume of CSK with 0.5% Triton X-100 at 4°C and centrifuged again at 100,000× ***g*** to pellet Triton X-100-insoluble material. The supernatant (TX100) was removed and the pellet from this spin resuspended in 2 ml SDS-PAGE sample buffer; the previous supernatants were brought to 2 ml with 2×SDS-PAGE sample buffer (Vogelmann and Nelson, 2007).

Continuous density-gradient centrifugation of homogenates from the embryonic rat telencephalon, followed by a quantitative analysis of proteins present in each fraction following western blot analysis was performed as described by Vogelmann and Nelson (Vogelmann and Nelson, 2007). Particles migrated in the gradient to a position that matched their density, with cytosolic proteins remaining in the densest bottom third of the gradient (fractions 16-21) and buoyant particles in the lighter upper two-thirds of the gradient (fractions 1-15; see Fig. S4 in the supplementary material). The protein concentration was determined for each fraction and then plotted in arbitrary units normalized to the maximum protein concentration (in fraction 17; see Fig. S4 in the supplementary material). In addition, markers for distinct subcellular compartments were used to distinguish fractions containing cytosol (actin), membranes derived from the Golgi apparatus (TGN38), and the plasma membrane (Cadherin, Na^+/K^+ ATPase; Fig. S4 in the supplementary material). Proteins from samples were separated by SDS-PAGE (Laemmli, 1970) and processed for western blotting (http://www.licor.com). The signal intensity of each band in western blots from each fraction was normalized to the maximal value obtained for each protein; these values were then plotted to represent the relative amount of protein present in each fraction from the gradient (see Fig. S4 in the supplementary material). Three independent gradients were analyzed for each study. Graphs of protein distribution throughout density gradients were generated using Microsoft Excel. Integrated intensity data and protein concentration for each set of fractions were converted linearly to arbitrary units from zero to maximum of 100.

In utero electroporation

In utero electroporation was performed as described (Kawauchi et al., 2003). Embryos were collected 2 or 5 days post-surgery for analysis; five embryos were analyzed for each time point.

Cell cycle analyses

For labeling index (LI) studies, pregnant mice were injected with BrdU at E11.5 or E13.5, and embryos were collected 2 hours later. The LI (fraction of VZ cells in S phase) was calculated by determining the fraction of VZ cells that were $BrdU^+$. A modified LI (a relative measure of cell-cycle length) was calculated by determining the fraction of $Ki67^+$ cycling cells that were $BrdU^+$. For quit fraction (QF) analyses, pregnant mice were injected with BrdU at E12.5 and embryos were collected 24 hours later (n=3 for each analysis). The QF was determined by dividing the number of $BrdU^+/Ki67^-$ cells by the total number of $BrdU^+$ cells.

RESULTS

Expression of MALS in progenitor cells of the developing neocortex

To explore the function of MALS in corticogenesis, we assessed the expression and localization of MALS in the rat neocortex. RT-PCR and in situ hybridization analyses revealed that although *MALS-3* is strongly expressed by NPCs at E14.5, *MALS-1* and *MALS-2* are not detected (see Fig. S1 in the supplementary material). Immunohistochemistry revealed that MALS-3 protein is localized to the apical domains of NPCs lining the lateral ventricle (Fig. 1J-L), and of many other cell types throughout the body (see Fig. S2 in the supplementary material). We characterized the temporal expression of MALS-3 and found that MALS-3 is expressed diffusely throughout the apicobasal extent of NPCs as early as E9.5 in VZ cells (Fig. 1D-F). By E11.5, MALS-3 staining is localized apically at the ventricular surface (Fig. 1G-I), where it is maintained throughout neurogenesis (Fig. 1J-L).

When we compared the localization of MALS with that of F-actin (concentrated near adherens junctions at the boundary of the basolateral and apical regions) (Chenn et al., 1998), we found that MALS-3 occupies a domain largely supra-apical to that of F-actin (Fig. 1E). En face views of the ventricular surface revealed that F-actin rings the apical endfeet of NPCs (Fig. 1C). MALS-3 overlaps partially with these F-actin rings, but is also seen in regions that are both more apical and continuous (Fig. 1C), suggesting that MALS-3 is distributed in a cup-like pattern at the apical ends of NPCs.

Comparison of the MALS-3 localization with that of other apically localized proteins [ZO1 (TJP1 – Mouse Genome Informatics), ZO2 (TJP2 – Mouse Genome Informatics), pan-cadherin, β-catenin, PALS1 and CRB3] (Calegari et al., 2005; Cappello et al., 2006; Imai et al., 2006) revealed partially or entirely overlapping apical expression domains (Fig. 1A,B; Fig. 2). Of particular interest was the overlapping expression with PALS1 (Fig. 2G-I), a protein that binds directly to MALS-3 via an L27 interaction domain. Thus, MALS-3 and several proteins with which it can interact biochemically are expressed in, and localized to, the apical domains of NPCs during neocortical development.

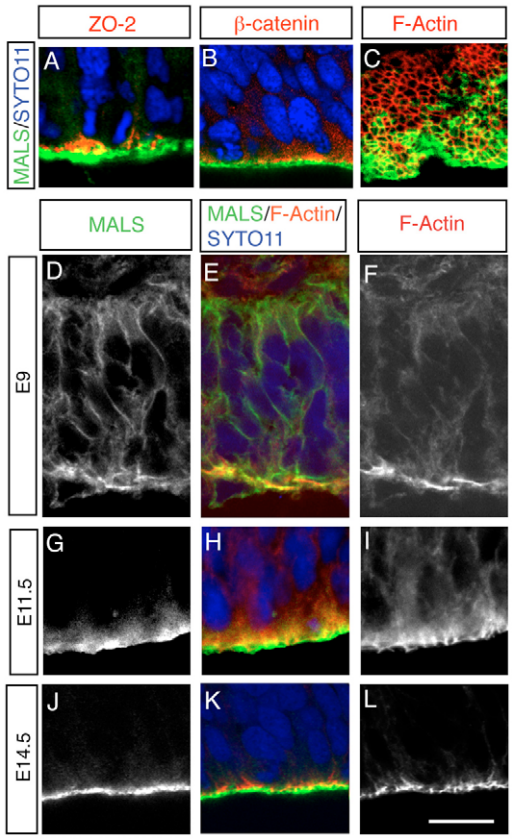

Fig. 1. MALS-3 is expressed by and localizes to the apical surface of NPCs. (**A-C**) Immunostaining of E14 coronal sections of rat telencephalon with antibodies against MALS-3 (green), ZO2, F-actin or β-catenin (red) reveal the supra-apical localization of MALS-3 relative to ZO2 (A), β-catenin (B) and F-actin (C). Nuclei are stained with SYTO-11 (blue). The en face view in C shows the lumen of the ventricle at the bottom, then (from bottom to top) passes through the apical-most ends of VZ cells and into the domain occupied by adherens junctions, which appear as circles of F-actin staining. (**D-L**) MALS-3 is initially localized diffusely in VZ cells (D-F), but appears to adopt an apical localization at the onset of neurogenesis (~E11.5, G-I), which is maintained throughout the rest of embryonic life (J-L). Scale bar: 5 μm.

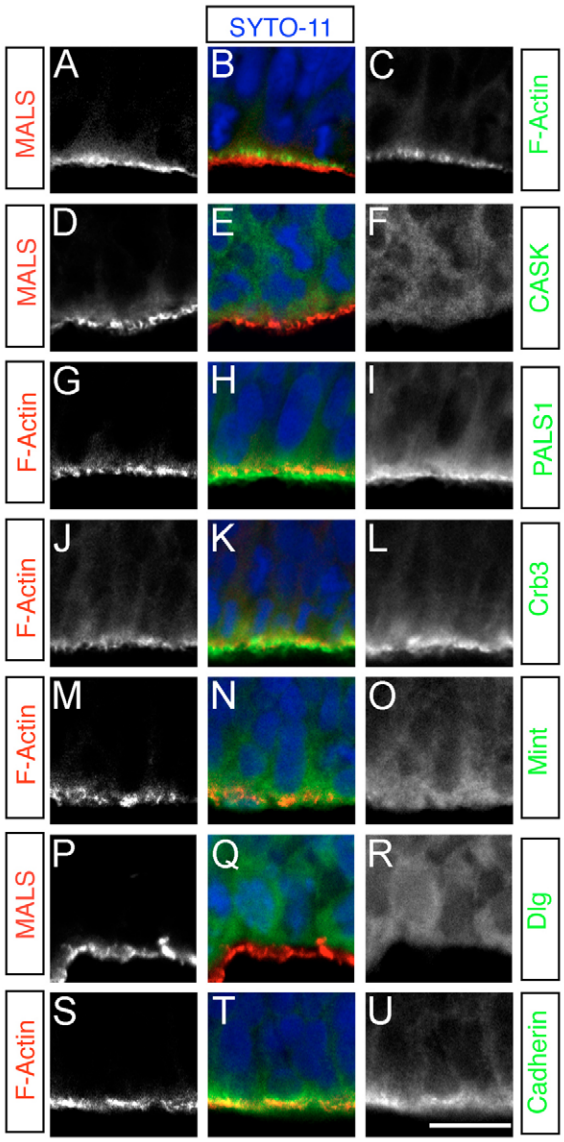

Fig. 2. Localization of MALS immunoreactivity compared with other proteins in the VZ. (**A-C**) Immunostaining of E14 coronal sections of rat telencephalon reveals that MALS is localized supra-apical to F-actin. (**D-F**) CASK antibody did not reveal specific immunostaining in the VZ. (**G-I**) PALS1 is also localized supra-apical to F-actin, in a pattern similar to that of MALS. (**J-L**) CRB3 localization is similar to that of PALS1 and MALS. (**M-O**) Mint shows a diffuse yet apically biased localization in the VZ. (**P-R**) DLG, a protein localized basolaterally in many cell types, does not localize to the apical surface in NPCs. (**S-U**) F-actin colocalized with staining for pan-cadherin in the apical domains of VZ cells. Scale bar: 5 μm.

MALS-3 is associated with cell membranes

Although MALS-3 does not contain a transmembrane domain, in other systems, it associates with membranes via interactions with other proteins (Roh and Margolis, 2003; Straight et al., 2006). To ascertain whether the MALS-3 in VZ cells is associated with the plasma membrane, we used high-speed centrifugation and density-gradient separation to separate membranes and membrane-associated proteins from the cytosol. High-speed centrifugation revealed that MALS-3 exists in two pools in the telencephalon: approximately two-thirds of the total MALS-3 was present in the cytosolic fraction (S100), whereas one-third was distributed between Triton-soluble (TX100) and Triton-insoluble (SDS) membranes (Fig. 3A). This suggests that a substantial fraction of the MALS-3 in NPCs is associated with membranes. To compare the distribution of MALS-3 with that of other proteins with which it might potentially interact, we probed the same fractions with antibodies against CASK, Mint (LIN-10; APBA1 – Mouse Genome Informatics), PALS1, and several apically localized proteins. These studies revealed that CASK is associated primarily with Triton-insoluble membranes, whereas Mint was found mostly in the cytosol (Fig. 3A). PALS1, DLG, β-catenin, cadherin and Na^+/K^+ ATPase were found primarily in membrane fractions, whereas p38γ/SAPK3 was almost exclusively in the cytosol (Fig. 3A).

To better quantitate these results, we performed density-gradient centrifugation of homogenates from embryonic rat telencephalon followed by a quantitative western blot analysis of proteins present in each fraction (Vogelmann and Nelson, 2007). Markers for distinct sub-cellular compartments were used to distinguish fractions containing cytosol, Golgi membranes and plasma membranes (see

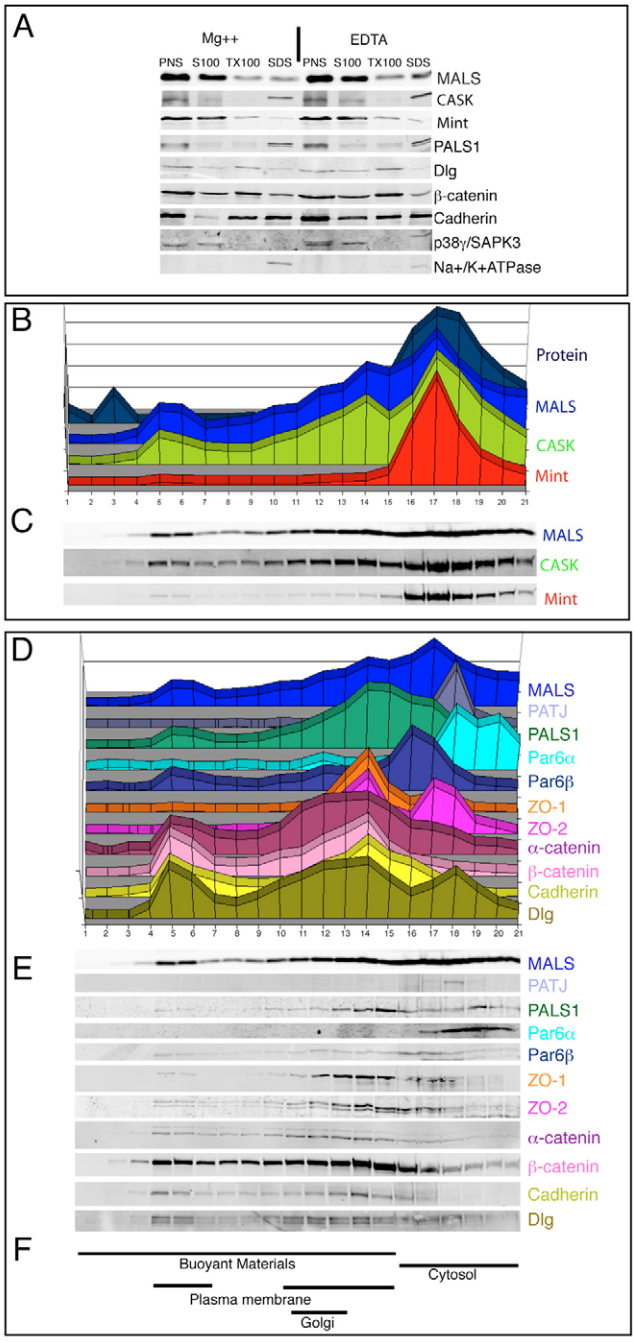

Fig. 3. Distribution of proteins between membrane and cytosol in the postnuclear supernatant. (**A**) Triton soluble membranes (TX100), triton insoluble membranes (SDS) and cytosol (S100) from E14 rat telencephalon homogenate postnuclear supernatant (PNS) were prepared with either magnesium ions (Mg^{2+} group) or a chelating agent (EDTA group), separated by SDS-PAGE, and visualized by western blot. The presence of either Mg^{2+} or EDTA resulted in no reproducible differences in the molecular distributions between cytosol, Triton soluble membranes and Triton insoluble membranes. (**B**,**C**) Integrated density plots of the distribution of MALS, CASK and Mint proteins in an iodixanol density gradient (B), with the corresponding western blots of the different fractions (C). The distributions of MALS and CASK showed a strong similarity. (**D**,**E**) Integrated density plots of the distribution of known cell polarity proteins (D), together with corresponding western blots (E), reveal the distribution of several cell polarity proteins found in NPCs. Taken together, the data suggest that MALS might interact with CASK and PALS1 in NPCs based on a similar cellular localization. (**F**) Bars represent the cellular distribution of proteins known to associate with different subcellular compartments (based on data shown in Fig. S4 in the supplementary material).

Fig. S4 in the supplementary material). The signal intensities of bands in western blots were normalized to the maximal value obtained for each protein then plotted to represent the relative amount of protein in each fraction from the gradient (Fig. S4 in the supplementary material). These experiments revealed that, as predicted from the high-speed centrifugation, MALS was present in both cytosolic fractions (peak, fraction 17) and fractions containing plasma membrane (fractions 5 and 14; Fig. 3B,C). MALS and CASK had nearly identical distributions, with an overall maximum at fraction 17, and local maxima at fractions 5 and 14 (Fig. 3B,C). These distributions suggest that CASK and MALS are each found in the cytosolic and plasma membrane pools, consistent with the possibility that these proteins interact biochemically. Mint was distributed in a single peak centered at fraction 17, suggesting that Mint is primarily cytosolic. Thus, in contrast to the close association between LIN-7, LIN-2, and LIN-10 in *C. elegans*, only MALS and CASK localize to plasma membranes in NPCs (although all three proteins might still interact in the cytosol).

Next, we examined the distributions of 10 proteins implicated in cell polarity and/or the formation of apically localized junctions. Collectively, these showed diverse behaviors during gradient centrifugation (Fig. 3D,E), but several were distributed across the gradient in patterns similar to that of MALS. PALS1, which interacts with MALS and is required for tight junction formation in MDCK cells (Hurd et al., 2003; Roh et al., 2002; Straight et al., 2004), exhibited a major peak at fraction 14 and a minor peak at fraction 5, and a broad distribution across cytosolic fractions. It is likely that MALS and PALS1 interact biochemically, as PALS1 can be co-immunoprecipitated with antibodies to MALS-3 (see Fig. S3C in the supplementary material). Interestingly, α-catenin, β-catenin and cadherin were similarly distributed in density gradients (Fig. 3D,E), suggesting that each is associated with plasma membranes.

The junctional proteins ZO1 and ZO2 had a major plasma membrane peak at fraction 14, but only ZO2 had a second peak in the cytosol (fraction 17; Fig. 3D,E). DLG, which is commonly considered to be basolaterally localized but is found at tight junctions in MDCK cells (Albertson and Doe, 2003; Peng et al., 2000), exhibited peaks in plasma membrane fractions 5 and 14, and cytosolic fraction 18. DLG co-immunoprecipitated with MALS-3 from these gradients (see Fig. S3C in the supplementary material), which is consistent with recent reports that DLG1 interacts with all three MALS proteins via associations with the PALS1 family member MPP7 (Bohl et al., 2007). The polarity proteins PAR6A and PAR6B were found primarily in cytosolic fractions, although PAR6B also displayed a small plasma membrane peak (fraction 5). Although previous studies suggest that PAR6B localizes to the cytosol in MDCK cells, and that PAR6A associates with the tight junction protein ZO1 (Gao and Macara, 2004), these relationships were not apparent from our study. Finally, PATJ was found almost exclusively in cytosolic fraction 18 (Fig. 3D). This is surprising because PATJ associates with tight junctions in MDCK cells (Shin et al., 2005), where it interacts with PALS1 (Roh et al., 2002; Straight et al., 2006) and Crumbs (Makarova et al., 2003).

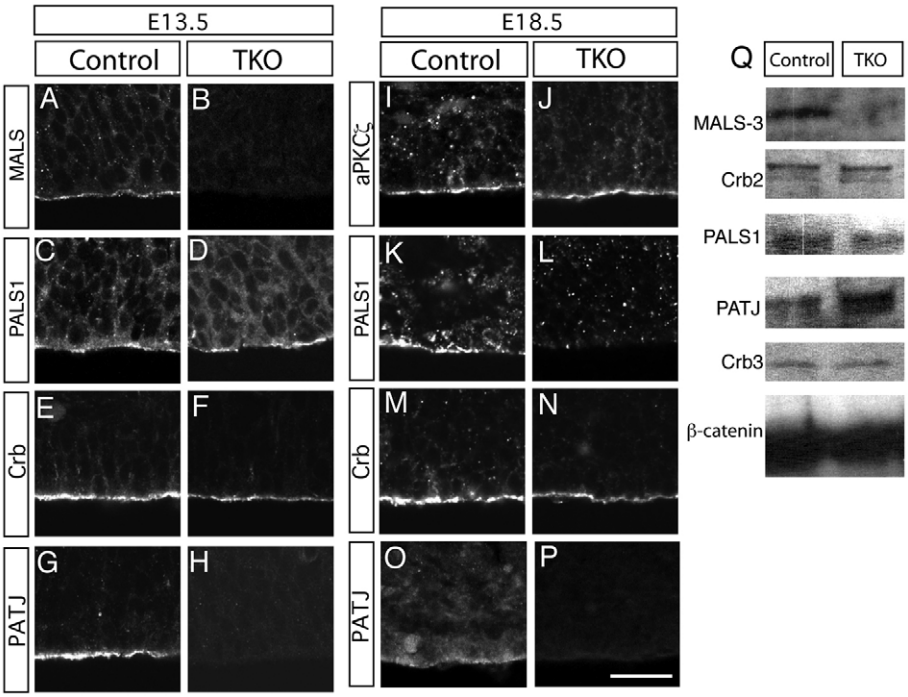

Fig. 4. MALS is required for the maintenance but not establishment of the apical localization of PALS1 and PATJ during corticogenesis.
(**A-H**) Coronal sections of control and *MALS*^{TKO} mutant brains at E13.5 immunostained for MALS (A,B), PALS1 (C,D), CRB (E,F) and PATJ (G,H) reveal loss of MALS (B) and apical PATJ (H) relative to control. Coronal sections of control and *MALS*^{TKO} mutant brains at E18.5 immunostained for aPKCζ (**I**,**J**), PALS1 (**K**,**L**), CRB (**M**,**N**) and PATJ (**O**,**P**) reveal loss of apical PALS1 (L) and PATJ (P) in *MALS*^{TKO} mutants. Scale bar: 10 μm. (**Q**) No changes were observed in total protein levels for any of the above proteins in *MALS*^{TKO} mutant brains relative to controls.

In sum, of the potential MALS interactors studied here, the distribution of CASK in density gradients was nearly identical to that of MALS, and the distribution of PALS1 was similar in lighter plasma membrane fractions. These observations are consistent with evidence that CASK and PALS1 interact with MALS in MDCK cells (Straight et al., 2006). In addition, analyses of homogenates from postnatal brains, in which MALS-1 and MALS-2 are found at synapses, have revealed that MALS associates with CASK, Mint and liprins in postmitotic neurons (Olsen et al., 2005a).

MALS triple-knockout mice show defects in the maintenance of apical polarity

Based on expression pattern and biochemistry, we hypothesized that MALS-3 might play a role in establishing and/or maintaining apical polarity early in neurogenesis. To test this, we examined corticogenesis in mice in which all three MALS genes were genetically disrupted (Olsen et al., 2005a). Mice that lack *MALS-1* and *MALS-2* appear normal, owing to the upregulation of *MALS-3* in neurons, and were therefore used as controls in our study. Mice in which only *MALS-3* is mutated also lack obvious defects, presumably because of compensation by the two other MALS isoforms (Misawa et al., 2001). MALS triple knockout (*MALS*^{TKO}) mice were bred and genotyped as described earlier (Olsen et al., 2005a). *MALS*^{TKO} pups die soon after birth (Olsen et al., 2005a), and examination of their brains at P0 revealed no obvious morphological abnormalities, such as smaller brain size or defects in cortical lamination (as evidenced by immunostaining with layer-specific antibodies; see Fig. S5 in the supplementary material).

Although it comprises less than 2% of the entire membrane surface (Huttner and Kosodo, 2005; Kosodo et al., 2004), the apical domain of NPCs represents a region that is actively targeted by several proteins, including signaling molecules such as β-catenin and aPKC (Chenn and Walsh, 2002; Chenn et al., 1998; Imai et al., 2006), and EGFR ((Sun et al., 2005). Because the MALS homolog LIN-7 plays an essential role in the basolateral targeting of EGF receptors in *C. elegans* vulval precursors (Kaech et al., 1998), we examined EGFR localization in *MALS*^{TKO} brains but observed no differences between controls and mutants (data not shown). Because MALS-3 regulates apicobasal polarity in MDCK cells, we hypothesized that MALS-3 might play a similar role in NPCs (Straight et al., 2006). At E13.5, the VZ appeared intact in *MALS*^{TKO} brains (Fig. 4A,B). However, *MALS*^{TKO} mutants showed a complete loss of PATJ staining (Fig. 4H), which is normally concentrated apically (Fig. 4G). The localization of other apical proteins, including PALS1, was unaltered (Fig. 4; data not shown) (Kamberov et al., 2000). The loss of PATJ staining by E13.5 was surprising as MALS-3 associates with PATJ through its interaction with PALS1, a part of the CRB3/PALS1/PATJ complex. Moreover, our density centrifugation experiments showed distinct patterns for MALS-3 and PATJ, suggesting that they occupy distinct intracellular domains (Fig. 3). Nevertheless, PATJ was completely absent from the apical region of *MALS*^{TKO} NPCs.

Similar analyses of E18.5 *MALS*^{TKO} mutants revealed that, in addition to the loss of PATJ apically (Fig. 4O,P), NPCs showed a loss of PALS1 immunoreactivity from their apical domains (Fig. 4K,L). This suggests that MALS-3 is not required for the initial apical targeting of PALS1 in NPCs but is important for maintaining its apical localization. In many mutants, the distribution of CRB appeared normal (Fig. 4M,N), but we occasionally observed a reduction in the intensity of apical CRB staining (data not shown). Because the antibody used to detect CRB3 also detects CRB2 (data not shown), it is possible that changes in the localization of one isoform might be masked if that of the other were unaltered. No changes were observed in the distributions of PAR3, PAR6 or aPKCζ (Fig. 4I,J; data not shown), suggesting that MALS does not affect the PAR6 signaling pathway in NPCs. Despite the loss of at least three proteins (MALS-3, PATJ, PALS1, and occasionally CRB) from the apical surface, the VZ still appeared intact at E18.5, suggesting that none of these proteins is crucial for maintaining the structural integrity of the VZ. Western blots revealed no obvious changes in the total

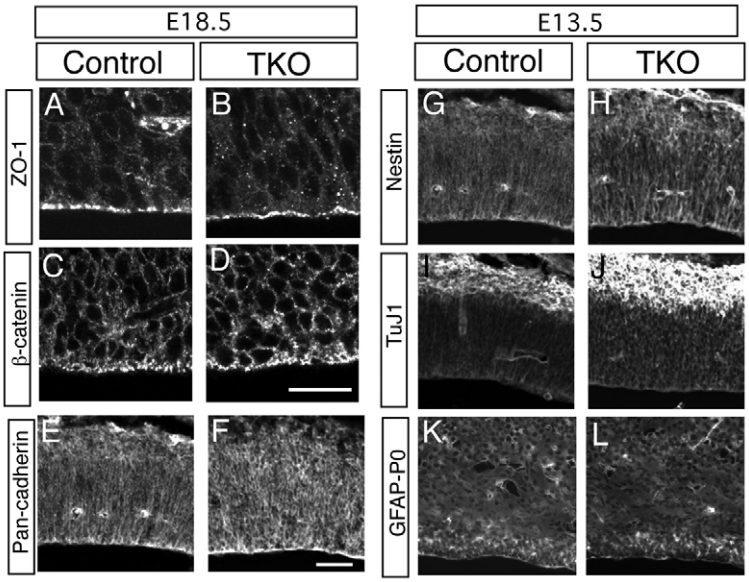

Fig. 5. Adherens junction integrity is not compromised in *MALS^{TKO}* embryos. (**A**,**B**) Coronal sections of E18.5 embryos immunostained for ZO1 to identify adherens junctions reveal normal staining in *MALS^{TKO}*. (**C-F**) Antibodies against β-catenin (C,D) and pan-cadherin (E,F), both of which localize to the apical surface at the adherens junctions, reveal no change in *MALS^{TKO}* mice relative to controls. (**G-L**) Coronal sections of E17.5 embryos stained with antibodies against nestin (G,H), to identify neural progenitors, and GFAP (K,L), to reveal glial cells, reveal no difference between *MALS^{TKO}* mice and controls. (I,J) However, antibodies against the neuronal marker TuJ1 reveal a broader TuJ1 staining pattern in the cortex of *MALS^{TKO}* embryos, suggesting that *MALS^{TKO}* progenitors quit cycling prematurely and differentiate into neurons. Scale bars: 10 μm.

protein levels of PALS1 or PATJ (Fig. 4Q), suggesting that MALS is required for the apical localization, but not the overall stability, of PALS1 and PATJ in NPCs. This result contrasts with studies in which silencing of *MALS-3/LIN-7* in MDCK cells resulted in a loss of PATJ from tight junctions because of altered protein stability (Straight et al., 2006).

Adherens junctions remain intact in *MALS^{TKO}* brains

In MDCK cells, the loss of PATJ by RNAi-mediated gene silencing leads to a loss of tight junctions, as revealed by the loss of ZO1 at these structures (Shin et al., 2005). Although NPCs in vivo do not form tight junctions (Aaku-Saraste et al., 1996), they do form adherens junctions where ZO1 and ZO2 colocalize. The intact appearance of the VZ in *MALS^{TKO}* embryos suggested that adherens junctions were maintained. This was confirmed by the continued expression of ZO1 and ZO2 in mutant embryos (Fig. 5A,B; data not shown). We also assessed the localization of cadherins, an integral component of adherens junctions, and the signaling protein β-catenin, as changes in the localization of the proteins would likely have profound consequences on NPCs (Chenn and Walsh, 2003). Again, no differences in protein localization were observed in the *MALS^{TKO}* cortex (Fig. 5C-F). Collectively, these results suggest that MALS is not required for the establishment or maintenance of adherens junctions in the developing brain.

Analysis of NPC proliferation and differentiation in *MALS^{TKO}* mice

To ascertain whether the loss of MALS-3 and, subsequently, PATJ and PALS1 altered neurogenesis, we immunostained brains with antibodies that distinguish NPCs (nestin), neurons (TuJ1, NeuN and TBR1) and glial cells (GFAP; see Fig. 5; data not shown). At E13.5, staining for nestin and GFAP appeared similar in mutant and control brains (Fig. 5G,H). However, we observed a broadened TuJ1 expression domain in *MALS^{TKO}* mutants compared with controls (Fig. 5I,J), suggesting that the production of neurons might be expanded or initiated prematurely in MALS mutants.

To ascertain whether the loss of MALS genes altered NPC proliferation, we first performed BrdU injections to assess the labeling index (LI, representing cells in S phase). At E11.5, the LI in *MALS^{TKO}* mice (0.36±0.05) was significantly lower than in controls (0.44±0.03, $P<0.03$; Fig. 6A). A reduction in LI suggests that either fewer VZ cells were cycling in the mutant, or the same number of cells were cycling more slowly. The limited availability of *MALS^{TKO}* mice precluded us from performing cumulative labeling studies to ascertain the total length of the cell cycle. Instead, we assessed BrdU incorporation in actively cycling cells only by immunostaining embryos for BrdU and Ki67 (expressed by all cycling cells). If the altered LI were due to decreased numbers of cycling cells, we should see no difference in fraction of Ki67$^+$ cells that were also BrdU$^+$ in mutants. However, if the decrease in LI arose from a lengthened cell cycle, fewer BrdU$^+$/Ki67$^+$ cells would be expected (Chenn and Walsh, 2003; Siegenthaler and Miller, 2005). Indeed, we observed a significant decrease in the fraction of Ki67$^+$ cells that were BrdU$^+$ (control, 0.80±0.04; *MALS^{TKO}*, 0.63±0.06; $P<0.01$), suggesting that MALS-deficient progenitors cycle more slowly than controls.

During early corticogenesis, wild-type NPCs divide rapidly and most divisions are symmetric, producing more progenitors; later, the cell cycle slows and the fraction of daughter cells that differentiate into neurons increases (Calegari et al., 2005). The lower LI in E11.5 *MALS^{TKO}* brains and the broadened domain of TuJ1 immunoreactivity suggested that early NPCs might prematurely enter the neurogenic phase of development. To assess the fraction of cells that differentiated following early divisions in *MALS^{TKO}* mutants, we calculated the Quit Fraction (QF) of cells that exited the cell cycle. The QF in *MALS^{TKO}* embryos (0.53±0.03) was significantly higher than in littermate controls (0.45±0.03, $P<0.03$; Fig. 6B), demonstrating that *MALS^{TKO}* progenitors differentiate prematurely during early neurogenesis. As the orientation of the mitotic spindle can affect the outcome of NPC divisions (Chenn and McConnell, 1995), we investigated whether the increase in neurogenic divisions was correlated with changes in spindle orientation. However, no significant differences in the orientations of E11.5 VZ cells in anaphase of the cell cycle were observed between control and *MALS^{TKO}* embryos (data not shown), suggesting that MALS-3 does not regulate neurogenesis by controlling mitotic spindle orientation.

Interestingly, *MALS^{TKO}* progenitors appeared to synchronize with their control counterparts by E13.5. BrdU injections at this age revealed no differences in the LI of *MALS^{TKO}* mice compared with

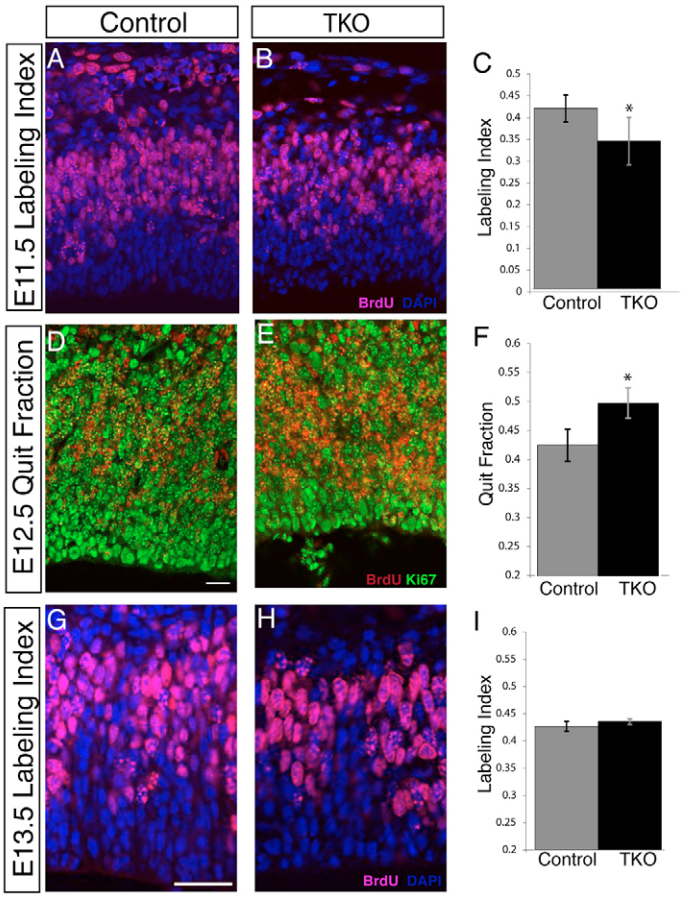

Fig. 6. *MALS^{TKO}* embryos display significant differences in labeling index and quit fraction during early neurogenesis. (**A-H**) Coronal sections of E11.5 (A,B), E12.5 (D,E) and E13.5 (G,H) *MALS^{TKO}* mutants and matching littermate control brains injected with BrdU 2 hours (A,B,G,H) or 24 hours (D,E) before sacrifice. Sections were immunostained with antibodies to BrdU (A,B,D,E,G,H) and Ki67 (D,E). (C) At E11.5, *MALS^{TKO}* progenitors have a lower labeling index (total number of BrdU$^+$ cells/total number of cells) than do controls. (F) A larger number of *MALS^{TKO}* mutant progenitors at E12.5 have quit the cell cycle relative to control littermates (BrdU$^+$ Ki67$^-$/total number of BrdU$^+$ cells). (**I**) *MALS^{TKO}* mutant progenitor cells recover normal cell-cycle dynamics just a day later at E13.5, at which time no differences in the labeling index are apparent. Scale bar: 10 μm.

controls (Fig. 6C). Thus, although the loss of MALS-3 alters NPC proliferation during early stages of neurogenesis, by mid-neurogenesis NPCs resumed normal cell cycle dynamics. We presume that this recovery explains the relatively normal size and appearance of the cortex in newborn *MALS^{TKO}* mice.

Deliberate mistargeting of MALS-3 results in a breakdown of the VZ

To ascertain whether the apical localization of MALS is required for its function, MALS-3 was tagged with an N-terminal myristoylation sequence (MGSSKSKPKDPS; *CA-myr_MALS-3*) and co-electroporated with *CA-EGFP* into the lateral ventricles of E13.5 embryos. As a control, full-length MALS-3 without a myristoylation tag (*CA-FL_MALS-3*) was electroporated into embryos in the contralateral uterus. To eliminate the possibility that expression of any myristoylated protein disrupts VZ cells, we electroporated embryos with a construct expressing myristoylated CRB3 (*CA-Myr_CRB3*). At E18.5, cortices electroporated with *CA-FL_MALS-3* appeared normal, with large numbers of EGFP$^+$ neurons and their axons present in the cortical plate (see Fig. S6A in the supplementary material). We observed no change in the localization of CRB3, PALS1 and aPKC in the VZ in these brains (Fig. 7A-C). Similarly, introduction of *CA-myr_CRB3* had no observable effect on the structure of the VZ or the localization of the apical proteins ZO1, PATJ and PALS1 (Fig. 7D,G,J), even though CRB protein itself was observed in the basolateral regions of EGFP$^+$ cells (Fig. 7M).

By contrast, embryos electroporated with *CA-myr_MALS-3* showed striking morphological abnormalities (Fig. 7P-R; see also Fig. S6C in the supplementary material). The integrity of the VZ was compromised, and the lateral ventricles were infiltrated with TuJ1$^+$ cells (Fig. 7R). Within 2 days of electroporation, at E15.5, breaks were observed in the apical staining patterns of ZO1 (Fig. 7E,F), PATJ (Fig. 7H,I), PALS1 (Fig. 7K,L) and CRB (Fig. 7N,O) near EGFP$^+$ cells, suggesting that adherens junctions were disrupted at these sites. Consistent with this interpretation, we also observed breaks in β-catenin staining (see Fig. S6C in the supplementary material). The ventricle contained misplaced cells that were positive for nestin at E15.5 (although in smaller numbers than at E18.5), suggesting they were delaminated NPCs (data not shown). These phenotypes are reminiscent of the conditional loss of β-catenin in the developing forebrain, in which adherens junction integrity is compromised, leading to a delamination of NPCs and the appearance of ectopic cells in the lateral ventricles (Junghans et al., 2005). Interestingly, we did not observe any changes in β-catenin localization in *MALS^{TKO}* brains (Fig. 4, Fig. 5C,D), suggesting that MALS-3 is not normally required for the apical localization of β-catenin.

Finally, we calculated the LI and QF for electroporated VZ cells at E14.5 (one day after electroporation) and E15.5, respectively. We observed no significant change in the QF upon expression of *CA-myr_MALS-3* (data not shown); however, the LI was significantly reduced in cells expressing *CA-myr_MALS-3* (0.31±0.06) compared with controls (0.55±0.04; $P<0.006$). Calculation of the fraction of Ki67$^+$ cells that incorporated BrdU revealed that cells expressing *CA-myr_MALS-3* also showed a significant reduction of the LI (0.39±0.06) compared with GFP$^+$ controls (0.67±0.01; $P<0.001$), indicating that the overexpression of *CA-myr-MALS-3* caused cells to cycle more slowly (as was observed in *MALS-3^{TKO}* mice). In conjunction with the changes in apical protein localization described above, these alterations in cell-cycle length suggest that *CA-myr-MALS-3* dominantly interferes with apicobasal polarity in NPCs.

DISCUSSION

MALS-3 is expressed by, and localizes apically within, cortical NPCs. We show that MALS-3 associates with cell membranes and interacts biochemically with CASK, Mint and PALS1 during corticogenesis. Genetic disruption of all three MALS genes in mice leads to an early loss of PATJ from the apical domain of NPCs, followed by a loss of PALS1 at later stages of neurogenesis. These findings suggest that MALS-3 is required for maintaining the apical localization of the CRB3/PALS1/PATJ complex. We observed no changes in adherens junction proteins, such as ZO1 or ZO2, or of the signaling proteins aPKCζ and β-catenin, suggesting that adherens junctions remained intact throughout corticogenesis. The loss of MALS genes also slowed the cell cycle and resulted in premature differentiation during early (but not later) stages of neurogenesis. These differences did not visibly alter the overall construction of the cortex, which appeared normal at P0. Finally, we found that

overexpression of a myristoylated form of MALS severely disrupted the apicobasal polarity of NPCs. Collectively, these data suggest that MALS is required for the maintenance of apicobasal polarity and the normal control of proliferation in the developing forebrain.

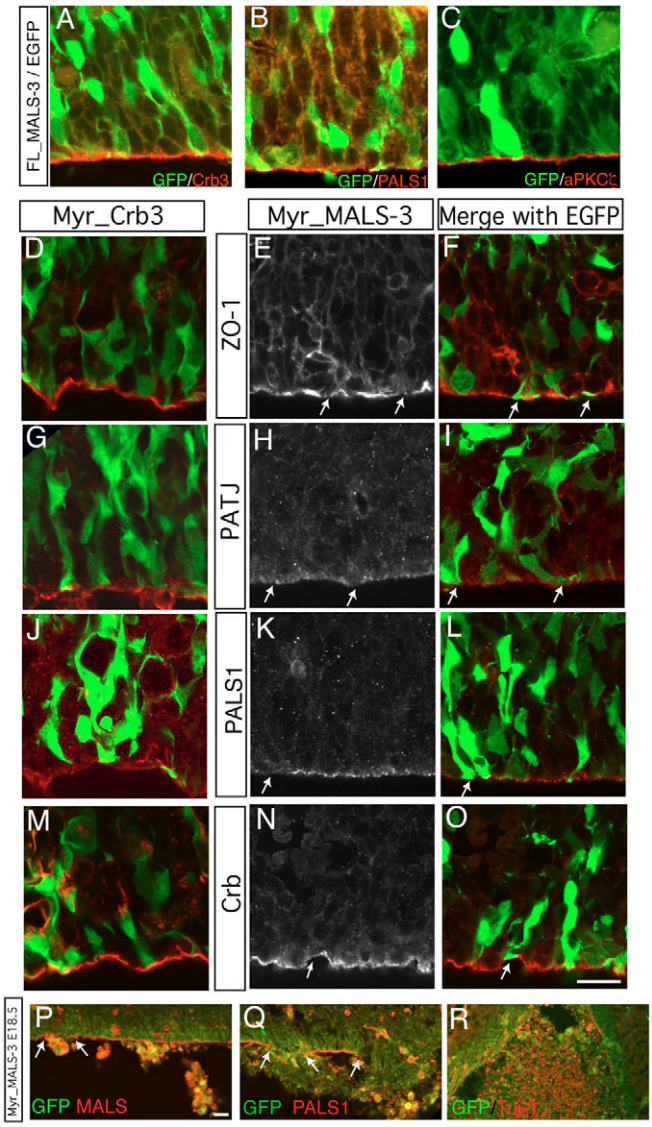

Fig. 7. The mislocalization of MALS-3 disrupts polarity. (**A-R**) Analyses of brains electroporated with *FL_MALS-3/EGFP* (A-C), *Myr_MALS-3* (E,F,H,I,K,L,N-R) or *Myr_CRB3* (D,G,J,M) at E13.5 and sacrificed at E15.5 (D-O) or E18.5 (P-R). Brains electroporated with *FL-MALS-3* show no changes in the apical localization of CRB3 (A), PALS1 (B) or aPKCζ (C). Brains electroporated with *Myr_CRB3* show no change in the apical localization of ZO1 (red, D), PATJ (red, G), or PALS1 (red, J) in GFP-positive cells (green). (M) CRB protein (red) is apparent in the basolateral regions of GFP-positive cells (green) following electroporation with *Myr_CRB3*, as expected. *Myr_MALS-3* electroporated, GFP-positive cells (green) show a loss of apical localization of ZO1 (E,F), PATJ (H,I) and PALS1 (K,L). CRB staining (red) appears reduced in some GFP-positive cells (N,O). At E18.5, *Myr_MALS-3* electroporated brains reveal misplaced cells in the lateral ventricles and breaks in the VZ, and MALS immunostaining is lost at those breaks (P). Larger breaks and loss of PALS1 staining (red) are also observed (Q). The ventricles are populated by delaminated cells that are TuJ1-positive (R). Arrows point to GFP-positive cells in the VZ that are not positive for ZO1 (E), PATJ (H), PALS1 (K), CRB (N), MALS (P) and PALS1 (Q). Scale bar: 10 μm.

MALS-3 is localized supra-apical to F-actin and associates with CASK, Mint and PALS1

The MALS homolog LIN-7 plays an essential role in the basolateral targeting of EGF receptors in *C. elegans* vulval precursors (Kaech et al., 1998). By contrast, in mammalian NPCs, MALS is localized apically, as is EGFR (Sun et al., 2005). However, MALS does not appear to regulate the apical targeting of EGFR in NPCs, as the distribution of EGFR was not obviously altered in mutants. This is perhaps not surprising in light of previous observations showing that EGFR is expressed during, and plays important functions only at later stages of, cortical development (Sun et al., 2005), compared with the earlier role for MALS demonstrated here.

It appears that the subcellular localization of MALS proteins is tissue dependent in vertebrates. For example, renal epithelial cells express all three MALS proteins, but their subcellular distributions vary among cell types, from primarily cytosolic in intercalated cells to predominantly basal or apical in the collecting ducts (Olsen et al., 2005b). By contrast, MDCK cells localize MALS-3/LIN7C, PALS1 and CRB3 to tight junctions (Roh and Margolis, 2003). It is not yet clear why MALS-3 and its partners show distinct localization patterns in different cell types; one possibility is that MALS-3 becomes localized to regions of cell-cell contact, including tight junctions in epithelial cells and adherens junctions in NPCs. However, in NPCs, MALS-3 clearly occupies a domain supra-apical to that of F-actin and adherens junctions. PALS1 is unlikely to mediate this localization because MALS-3 expression is not altered in MDCK cells silenced for PALS1 (Straight et al., 2004). One possibility is that β-catenin mediates the junctional localization of MALS-3, as β-catenin appears to be involved in actively localizing MALS-3 from the cytosol to calcium-mediated cadherin junctions in MDCK cells, and to early synapses in hippocampal neurons (Perego et al., 2000).

Many MALS-3 biochemical partners appear to be highly conserved in NPCs. In MDCK cells, MALS-3 stabilizes the PALS1 complex at tight junctions; cells silenced for MALS-3 lose the apical localization of PALS1 and ZO1, which delays the formation of tight junctions (Straight et al., 2006). This phenotype was fully rescued by introducing exogenous PALS1, providing strong evidence that MALS-3 function is mediated by PALS1. This interaction is not reciprocal, as MALS-3 expression is maintained in the absence of PALS1 (Straight et al., 2004). Consistent with these previous studies, $MALS^{TKO}$ VZ cells also showed a loss of PALS1, but only at later stages of neurogenesis. This suggests that MALS-3 is required not for the initial localization but for the maintenance of PALS1 apically in NPCs. We observed an earlier loss of apical PATJ from the apical surfaces of VZ cells, which was surprising in the absence of direct biochemical interactions between these two proteins. The loss of MALS did not appear to affect the expression levels of PALS1 or PATJ, suggesting that MALS-3 is primarily involved in maintaining the apical localization of the PALS1 complex. By contrast, MDCK cells silenced for LIN7C (MALS-3) displayed a loss of both PALS1 and PATJ owing to rapid protein turnover. The authors speculated that MALS-3/LIN7C is required to stabilize PALS1 apically. Because PATJ interacts with PALS1, the loss of PALS1 might result in the loss of PATJ from these cells (Straight et al., 2006). However, our data from $MALS^{TKO}$ mutant brains suggest that the role for MALS in apical protein localization can be separated from its role in protein stabilization.

In contrast to the role of MALS in maintaining polarity, PALS1 appears to play a crucial role in establishing apicobasal polarity. In MDCK cells, PALS1 is required for the formation of both tight and adherens junctions (Wang et al., 2007). These observations, together

with data from MDCK cells silenced for LIN7C/MALS-3 (Straight et al., 2006), provide strong evidence that PALS1 functions upstream of MALS-3, and that PALS1 can compensate to a large extent for the loss of MALS-3 during cell polarization. As we did not observe a loss of PALS1 from the apical surfaces of NPCs until later stages of corticogenesis, we suspect that PALS1 compensated functionally for the loss of MALS-3. On the basis of these observations, we would predict that the loss of *PALS1* in NPCs should generate a more profound disruption of corticogenesis than does the loss of all three MALS genes.

NPC proliferation and differentiation depend on apicobasal polarity but not the integrity of adherens junctions during cortical development

The relationship between apicobasal polarity and cell-cell junctions in controlling NPC proliferation has been a subject of recent interest, particularly in light of the role of junctions in mediating intercellular signaling. In *Drosophila*, intact junctions are essential for normal NPC proliferation (Lu et al., 2001); however, this requirement appears to be less strict in vertebrate neurogenesis. For example, loss of the Rho family GTPase *CDC42* results in a loss of adherens junctions and the mislocalization of mitotic progenitors from the apical to the basal region of the cortical VZ; however, misplaced cells continued to cycle despite their aberrant positions (Cappello et al., 2006). Similarly, conditional mutations of *aPKCλ* (a key component of the apically localized PAR complex) produced a complete loss of adherens junctions yet failed to disrupt neurogenesis (Imai et al., 2006). These observations suggest that maintenance of adherens junctions is not absolutely required for normal NPC proliferation.

In the $MALS^{TKO}$ mutants, we observed a complementary situation. Adherens junctions were intact in mutants, demonstrating that MALS-3 is not required for assembling or maintaining these junctions. However, we observed significant abnormalities in both the proliferation and differentiation of NPCs. First, $MALS^{TKO}$ mutants exhibited a lower LI and a lengthening of the cell cycle at the onset of corticogenesis, although proliferation recovered a few days later. Second, $MALS^{TKO}$ mutants displayed premature neuronal differentiation at early times during neurogenesis. Interestingly, these alterations were also temporary: the cortex as a whole appeared relatively normal at P0, and $MALS^{TKO}$ mutants did not display gross morphological changes, such as smaller brain size or loss of select neuronal populations, at birth.

Although these transient changes in proliferation present a puzzle, we note that, in normal animals, the transition from diffuse basolateral to strictly apical localization of MALS-3 occurs at ~E11.5, the same time at which we observed abnormal proliferation in mutant NPCs. We hypothesize that early NPCs are particularly vulnerable to alterations in the composition of their apical complexes, and that, at later stages, other apical polarity proteins restore normal patterns of proliferation. We further hypothesize that the higher QF observed at E13 is a result of the earlier shift in LI. Previous studies suggest that lengthening the cell cycle in NPCs can cause a shift from proliferative to neuron-generating divisions (Calegari et al., 2005). Thus, the more slowly cycling progenitors in E11 $MALS^{TKO}$ mice might differentiate into neurons earlier than control counterparts once they complete their cell cycle, thus generating a higher QF by E13.

In some mutant lines, higher QFs can be accompanied by a loss of NPCs, depleting the progenitor pool and reducing brain sizes owing to a loss of later-born neurons and/or glial cells. For example, loss of the chromatin remodeling protein BRG1 leads to precocious differentiation, a premature depletion of NPCs prior to gliogenesis, and a severe loss of glial cells (Lu et al., 2001). Gliogenesis, however, appeared normal in $MALS^{TKO}$ mice, further emphasizing that the consequences of altered QFs at E13.5 were subtle, most likely because of the rapid recovery in NPC proliferation.

It is not clear how the loss of MALS causes a shift towards neuronal differentiation at early stages of cortical development. One possibility is that MALS-3 is important for the asymmetric distribution or localization of a cell-fate determinant that regulates NPC proliferation and/or differentiation. For example, in epithelial cells, the tight junction protein ZO1 influences the G1/S-phase transition by sequestering a complex formed by CDK4 and the transcription factor ZONAB (Csda – Mouse Genome Informatics) away from the nucleus (Balda et al., 2003; Sourisseau et al., 2006). It is plausible that the disruption of MALS proteins in NPCs disrupts the localization of similar cell-cycle regulators, and thus leads to premature cell-cycle exit, although the molecular mechanisms underlying this phenomenon are as yet unknown.

Deliberate mistargeting of MALS-3 results in a breakdown of VZ integrity

Although a complete loss of MALS-3 did not affect the structural integrity of the VZ or intercellular junctions, the overexpression of MALS-3 tagged with an N-terminal myristoylation sequence profoundly altered the localization of PALS1 and PATJ, and triggered a loss of adherens junction proteins. The mislocalization of MALS-3 also resulted in a slowing of the cell cycle, suggesting that the myristoylated MALS-3 dominantly interfered with proliferation. Many electroporated cells delaminated from the VZ and spilled into the lateral ventricles, suggesting that the integrity of the adherens junctions was severely compromised by the mislocalization of MALS-3. We suspect that this mislocalization directly affects the localization of other proteins, particularly the MALS-3 direct-binding partner PALS1, but also the aPKC and PAR proteins, which require PALS1 for their normal localization (Margolis and Borg, 2005). Loss of these proteins from the apical surface might trigger the dissolution of adherens junctions (Imai et al., 2006), which could lead to the delamination of NPCs. However, $MALS^{TKO}$ mutant brains showed no alteration in aPKC staining, suggesting that MALS-3 is not required for the normal localization of the PAR3/PAR6/aPKC complex. Collectively, these results suggest that, although a loss of MALS-3 is tolerated by NPCs, its mislocalization is not, with mislocalization causing far more detrimental effects on apical polarity.

We thank W. James Nelson and Ben Margolis for sharing their expertise and reagents; Christine Kaznowski for technical support; Yoshima Takai for MALS cDNA constructs; Thomas Sudhof for MALS-3 and Mint GST fusion constructs; Ben Margolis for MALS, PALS1 and CRB3 antibodies; Andre Le Bivic for PATJ antibodies; Sandra Martin for the pCA vector; and W. James Nelson, Jennifer Shieh and Dino Leone for comments on the manuscript. Supported by NIH R01 MH51864.

Supplementary material

Supplementary material for this article is available at
http://dev.biologists.org/cgi/content/full/135/10/1781/DC1

References

Aaku-Saraste, E., Hellwig, A. and Huttner, W. B. (1996). Loss of occludin and functional tight junctions, but not ZO-1, during neural tube closure-remodeling of the neuroepithelium prior to neurogenesis. *Dev. Biol.* **180**, 664-679.

Albertson, R. and Doe, C. Q. (2003). Dlg, Scrib and Lgl regulate neuroblast cell size and mitotic spindle asymmetry. *Nat. Cell. Biol.* **5**, 166-170.

Astrom, K. E. and Webster, H. D. (1991). The early development of the neopallial wall and area choroidea in fetal rats. A light and electron microscopic study. *Adv. Anat. Embryol. Cell Biol.* **123**, 1-76.

Balda, M. S., Garrett, M. D. and Matter, K. (2003). The ZO-1-associated Y-box factor ZONAB regulates epithelial cell proliferation and cell density. *J. Cell Biol.* **160**, 423-432.
Bohl, J., Brimer, N., Lyons, C. and Vande Pol, S. B. (2007). The stardust family protein MPP7 forms a tripartite complex with LIN7 and DLG1 that regulates the stability and localization of DLG1 to cell junctions. *J. Biol. Chem.* **282**, 9392-9400.
Calegari, F., Haubensak, W., Haffner, C. and Huttner, W. B. (2005). Selective lengthening of the cell cycle in the neurogenic subpopulation of neural progenitor cells during mouse brain development. *J. Neurosci.* **25**, 6533-6538.
Cappello, S., Attardo, A., Wu, X., Iwasato, T., Itohara, S., Wilsch-Brauninger, M., Eilken, H. M., Rieger, M. A., Schroeder, T. T., Huttner, W. B. et al. (2006). The Rho-GTPase cdc42 regulates neural progenitor fate at the apical surface. *Nat. Neurosci.* **9**, 1099-1107.
Chen, B., Schaevitz, L. R. and McConnell, S. K. (2005). Fezl regulates the differentiation and axon targeting of layer 5 subcortical projection neurons in cerebral cortex. *Proc. Natl. Acad. Sci. USA* **102**, 17184-17189.
Chenn, A. and McConnell, S. K. (1995). Cleavage orientation and the asymmetric inheritance of Notch1 immunoreactivity in mammalian neurogenesis. *Cell* **82**, 631-641.
Chenn, A. and Walsh, C. A. (2002). Regulation of cerebral cortical size by control of cell cycle exit in neural precursors. *Science* **297**, 365-369.
Chenn, A. and Walsh, C. A. (2003). Increased neuronal production, enlarged forebrains and cytoarchitectural distortions in β-catenin overexpressing transgenic mice. *Cereb. Cortex* **13**, 599-606.
Chenn, A., Zhang, Y. A., Chang, B. T. and McConnell, S. K. (1998). Intrinsic polarity of mammalian neuroepithelial cells. *Mol. Cell. Neurosci.* **11**, 183-193.
Fish, J. L., Kosodo, Y., Enard, W., Paabo, S. and Huttner, W. B. (2006). Aspm specifically maintains symmetric proliferative divisions of neuroepithelial cells. *Proc. Natl. Acad. Sci. USA* **103**, 10438-10443.
Gao, L. and Macara, I. G. (2004). Isoforms of the polarity protein par6 have distinct functions. *J. Biol. Chem.* **279**, 41557-41562.
Gotz, M. and Huttner, W. B. (2005). The cell biology of neurogenesis. *Nat. Rev. Mol. Cell. Biol.* **6**, 777-788.
Hurd, T. W., Gao, L., Roh, M. H., Macara, I. G. and Margolis, B. (2003). Direct interaction of two polarity complexes implicated in epithelial tight junction assembly. *Nat. Cell Biol.* **5**, 137-142.
Huttner, W. B. and Kosodo, Y. (2005). Symmetric versus asymmetric cell division during neurogenesis in the developing vertebrate central nervous system. *Curr. Opin. Cell Biol.* **17**, 648-657.
Imai, F., Hirai, S., Akimoto, K., Koyama, H., Miyata, T., Ogawa, M., Noguchi, S., Sasaoka, T., Noda, T. and Ohno, S. (2006). Inactivation of aPKClambda results in the loss of adherens junctions in neuroepithelial cells without affecting neurogenesis in mouse neocortex. *Development* **133**, 1735-1744.
Junghans, D., Hack, I., Frotscher, M., Taylor, V. and Kemler, R. (2005). β-catenin-mediated cell-adhesion is vital for embryonic forebrain development. *Dev. Dyn.* **233**, 528-539.
Kaech, S. M., Whitfield, C. W. and Kim, S. K. (1998). The LIN-2/LIN-7/LIN-10 complex mediates basolateral membrane localization of the C. elegans EGF receptor LET-23 in vulval epithelial cells. *Cell* **94**, 761-771.
Kamberov, E., Makarova, O., Roh, M., Liu, A., Karnak, D., Straight, S. and Margolis, B. (2000). Molecular cloning and characterization of Pals, proteins associated with mLin-7. *J. Biol. Chem.* **275**, 11425-11431.
Kawauchi, T., Chihama, K., Nabeshima, Y. and Hoshino, M. (2003). The in vivo roles of STEF/Tiam1, Rac1 and JNK in cortical neuronal migration. *EMBO J.* **22**, 4190-4201.
Klezovitch, O., Fernandez, T. E., Tapscott, S. J. and Vasioukhin, V. (2004). Loss of cell polarity causes severe brain dysplasia in Lgl1 knockout mice. *Genes Dev.* **18**, 559-571.
Kosodo, Y., Roper, K., Haubensak, W., Marzesco, A. M., Corbeil, D. and Huttner, W. B. (2004). Asymmetric distribution of the apical plasma membrane during neurogenic divisions of mammalian neuroepithelial cells. *EMBO J.* **23**, 2314-2324.
Laemmli, U. K. (1970). Cleavage of structural proteins during the assembly of the head of bacteriophage T4. *Nature* **227**, 680-685.
Lu, B., Roegiers, F., Jan, L. Y. and Jan, Y. N. (2001). Adherens junctions inhibit asymmetric division in the Drosophila epithelium. *Nature* **409**, 522-525.
Makarova, O., Roh, M. H., Liu, C. J., Laurinec, S. and Margolis, B. (2003). Mammalian Crumbs3 is a small transmembrane protein linked to protein associated with Lin-7 (Pals1). *Gene* **302**, 21-29.
Margolis, B. and Borg, J. P. (2005). Apicobasal polarity complexes. *J. Cell Sci.* **118**, 5157-5159.
Misawa, H., Kawasaki, Y., Mellor, J., Sweeney, N., Jo, K., Nicoll, R. A. and Bredt, D. S. (2001). Contrasting localizations of MALS/LIN-7 PDZ proteins in brain and molecular compensation in knockout mice. *J. Biol. Chem.* **276**, 9264-9272.
Miyata, T., Kawaguchi, A., Okano, H. and Ogawa, M. (2001). Asymmetric inheritance of radial glial fibers by cortical neurons. *Neuron* **31**, 727-741.
Noctor, S. C., Flint, A. C., Weissman, T. A., Dammerman, R. S. and Kriegstein, A. R. (2001). Neurons derived from radial glial cells establish radial units in neocortex. *Nature* **409**, 714-720.
Olsen, O., Moore, K. A., Fukata, M., Kazuta, T., Trinidad, J. C., Kauer, F. W., Streuli, M., Misawa, H., Burlingame, A. L., Nicoll, R. A. et al. (2005a). Neurotransmitter release regulated by a MALS-liprin-alpha presynaptic complex. *J. Cell Biol.* **170**, 1127-1134.
Olsen, O., Wade, J. B., Morin, N., Bredt, D. S. and Welling, P. A. (2005b). Differential localization of mammalian Lin-7 (MALS/Veli) PDZ proteins in the kidney. *Am J. Physiol. Renal Physiol.* **288**, F345-F352.
Olsen, O., Moore, K. A., Nicoll, R. A. and Bredt, D. S. (2006). Synaptic transmission regulated by a presynaptic MALS/Liprin-alpha protein complex. *Curr. Opin. Cell Biol.* **18**, 223-227.
Peng, C. Y., Manning, L., Albertson, R. and Doe, C. Q. (2000). The tumour-suppressor genes lgl and dlg regulate basal protein targeting in Drosophila neuroblasts. *Nature* **408**, 596-600.
Perego, C., Vanoni, C., Massari, S., Longhi, R. and Pietrini, G. (2000). Mammalian LIN-7 PDZ proteins associate with beta-catenin at the cell-cell junctions of epithelia and neurons. *EMBO J.* **19**, 3978-3989.
Petersen, P. H., Zou, K., Hwang, J. K., Jan, Y. N. and Zhong, W. (2002). Progenitor cell maintenance requires numb and numblike during mouse neurogenesis. *Nature* **419**, 929-934.
Roh, M. H. and Margolis, B. (2003). Composition and function of PDZ protein complexes during cell polarization. *Am. J. Physiol. Renal Physiol.* **285**, F377-F387.
Roh, M. H., Makarova, O., Liu, C. J., Shin, K., Lee, S., Laurinec, S., Goyal, M., Wiggins, R. and Margolis, B. (2002). The Maguk protein, Pals1, functions as an adapter, linking mammalian homologues of Crumbs and Discs Lost. *J. Cell Biol.* **157**, 161-172.
Shin, K., Straight, S. and Margolis, B. (2005). PATJ regulates tight junction formation and polarity in mammalian epithelial cells. *J. Cell Biol.* **168**, 705-711.
Siegenthaler, J. A. and Miller, M. W. (2005). Transforming growth factor beta 1 promotes cell cycle exit through the cyclin-dependent kinase inhibitor p21 in the developing cerebral cortex. *J. Neurosci.* **25**, 8627-8636.
Sourisseau, T., Georgiadis, A., Tsapara, A., Ali, R. R., Pestell, R., Matter, K. and Balda, M. S. (2006). Regulation of PCNA and cyclin D1 expression and epithelial morphogenesis by the ZO-1-regulated transcription factor ZONAB/DbpA. *Mol. Cell. Biol.* **26**, 2387-2398.
Straight, S. W., Shin, K., Fogg, V. C., Fan, S., Liu, C. J., Roh, M. and Margolis, B. (2004). Loss of PALS1 expression leads to tight junction and polarity defects. *Mol. Biol. Cell* **15**, 1981-1990.
Straight, S. W., Pieczynski, J. N., Whiteman, E. L., Liu, C. J. and Margolis, B. (2006). Mammalian lin-7 stabilizes polarity protein complexes. *J. Biol. Chem.*
Sun, Y., Goderie, S. K. and Temple, S. (2005). Asymmetric distribution of EGFR receptor during mitosis generates diverse CNS progenitor cells. *Neuron* **45**, 873-886.
Vogelmann, R. and Nelson, W. J. (2007). Separation of cell-cell adhesion complexes by differential centrifugation. *Methods Mol. Biol.* **370**, 11-22.
Wang, Q., Chen, X. W. and Margolis, B. (2007). PALS1 regulates E-cadherin trafficking in mammalian epithelial cells. *Mol. Biol. Cell* **18**, 874-885.
Wodarz, A. and Huttner, W. B. (2003). Asymmetric cell division during neurogenesis in Drosophila and vertebrates. *Mech. Dev.* **120**, 1297-1309.
Zhong, W., Feder, J. N., Jiang, M. M., Jan, L. Y. and Jan, Y. N. (1996). Asymmetric localization of a mammalian numb homolog during mouse cortical neurogenesis. *Neuron* **17**, 43-53.